JEE Journal of Ecological Engineering

Journal of Ecological Engineering, 2027, 28(1), 155–171
https://doi.org/10.12911/22998993/241786
ISSN 2299–8993, License CC-BY 4.0

Received: 2026.09.25
Accepted: 2026.11.16
Published: 2026.12.01

Bounding bioretention storage requirements with inflow timing and duration summaries

Carlos Esteban Reyes Sánchez[1*], Xiomara Ayquel Bastidas Sánchez[1*], Luis Alberto Merchán Mosquera[2], Lisbet Geomara Lazo Arce[3], Dixie Marisol Lopezdomínguez Rivas[4], Carlos Alberto Bastidas Vaca[5]

[1] Facultad de Ciencias e Ingenierías, Universidad Estatal de Milagro, Milagro, Ecuador
[2] Facultad de Ciencias Matemáticas y Físicas, Universidad de Guayaquil, Guayaquil, Ecuador
[3] Instituto Europeo de Posgrado, España
[4] Facultad de Ingeniería Química, Universidad de Guayaquil, Guayaquil, Ecuador
[5] Facultad Ciencias Sociales, Educación Comercial y Derecho, Universidad Estatal de Milagro, Milagro, Ecuador
* Corresponding author's e-mail: xbastidass@unemi.edu.ec

ABSTRACT

Block averaging can hide the inlet pulses that determine surface ponding in bioretention systems. We asked what information must accompany the averages to keep the storage requirement within known limits. We derived bounds for a constant-outflow store and evaluated them in 776 new hydraulic model runs, including controlled pulse experiments; 22 monitored six-minute inlet records provided the main forcing. With an outflow equivalent to 30 mm/h over 1.800 m², four-hour averaging underestimated required storage by a median 89.2% among 13 records requiring more than 1 m³. Retaining two values—the largest positive and negative cumulative departures from the block averages—reduced the median conservative storage estimate from 6.50 to 1.75 times the six-minute requirement. These values bound averaging error, but they cannot determine storage: in a controlled layered-model experiment, two inflows with identical block volumes, peaks and reported extrema produced maximum surface depths of 130.25 and 82.74 mm. Maximum inflow volumes over nine selected durations provided a lower bound that complemented the upper error bound. Together, the bounds enclosed required storage for every tested record under constant outflow. With one-hour averages at 30 mm/h, the median ratio of the upper to lower bound was 1.29. The resulting interval identifies when summarized inflow supports sizing and when the available information leaves the requirement unresolved.

Keywords: bioretention, inflow reporting, required storage, temporal averaging, numerical experiments, duration–volume envelope.

INTRODUCTION

Bioretention design depends on the timing of inflow as well as its volume. A short pulse may create surface ponding while the same water, spread over several hours, infiltrates without accumulating above the soil. When an inlet hydrograph is replaced by block averages or event summaries, the design question is which retained fields bound the change in required storage and which can recover that requirement.

The International Stormwater BMP database requests event flow volume and peak flow, alongside rainfall depth and maximum one-hour intensity (Wright Water Engineers, Inc. & Geosyntec Consultants, 2019). Washington's TAPE guidance combines event summaries with hydrographs and flow logging every five minutes or less (Howie & Milesi, 2026).

The BMP database also acknowledges that event totals do not resolve within-event processes (Geosyntec Consultants & Wright Water

Engineers, Inc., 2011). We evaluate those volume-and-peak fields over inflow episodes, alongside prescribed 30–240 min blocks as a controlled resolution experiment. The latter are not presented as monitoring requirements or substitutes for the TAPE hydrograph.

Rainfall-resolution effects on urban runoff and drainage are well established (Bruni et al., 2015; Cristiano et al., 2017), and their magnitude varies with the model and response variable (Huang et al., 2019). At a fixed rainfall depth, frontal and conventional design-storm profiles produced different detention-storage trajectories (Burns et al., 2026). The consequences of simplifying rainfall and outlet representations have also been reviewed for detention design (Sambito et al., 2026). These studies establish sensitivity to temporal loading. They leave a separate reporting question: what design statement remains justified when only specified inflow summaries are retained?

Bioretention models represent interactions among surface, soil and drainage-layer water (De-Ville et al., 2025; Lisenbee et al., 2021). Field monitoring distinguishes hydrologic performance and flow-regime effects (Bonneau et al., 2020), while model-based assessments quantify parameter uncertainty (Gomes et al., 2023). Input resolution and numerical integration step have different effects on hydrological performance (Tudaji et al., 2025a, 2025b). Characteristic-timescale analysis also relates storm forcing to low-impact-development response (Castro et al., 2025). A reporting assessment must separate these hydraulic effects from information removed before the model is run.

Reflected-storage bounds and the duration–volume representation have established foundations in queueing theory (Kruk et al., 2007; Le Boudec and Thiran, 2001). Building on those results, this study constructs attainable error envelopes for specified block summaries and applies them to storage decisions. Volumes and peaks determine worst-case margins, residual extrema retain the exact input-discrepancy bound, and selected duration maxima supply a complementary lower bound. Their combination identifies whether a stated capacity is sufficient, insufficient or unresolved under the declared hydraulic assumptions.

The objectives are to quantify storage margins from retained inflow fields, derive checks for a chosen storage capacity or error tolerance, and combine block summaries with duration maxima to bound required storage under constant outflow. The 22 public Wicks Reserve inlet records serve only as forcing: the storage comparisons reported here come from new analytic calculations and 776 model executions, and no previously published results are reanalysed.

MATERIALS AND METHODS

Study design and data generated

The study generates analytical and numerical results in three components. First, the reporting envelopes, operational checks and combined interval (Equations 5–9 and 11) are derived for this work from established comparison and duration–volume results (Equations 4 and 10), with proofs in Supplementary Sections S1–S6, S12, S14 and S15. Second, these results were evaluated for 88 record–interval combinations, 66 record–outflow comparisons and 264 record–outflow–block interval tests. Third, 776 model executions were performed: 330 layered-model runs forced by the monitored records, 330 corresponding runs with a 300 mm berm, 14 controlled-input runs, 36 diagnostic executions and 66 antecedent-wetness runs. The only measured forcing data are the 22 six-minute inlet records of the Wicks Reserve dataset (Bonneau, Fletcher, et al., 2021); no results from previous publications are reanalysed. All generated numerical data are archived with the analysis code (see Data and code availability).

Monitoring records and inlet reconstruction

The forcing inputs are the 22 six-minute inlet records of the Wicks Reserve monitoring dataset (Bonneau, Fletcher, et al., 2021). All 22 files matched their MD5 checksums. Required flow channels were complete, intervals regular and records non-overlapping (Table 1). Despite varying headers, reconstruction uses only timestamps and the small-inlet, large-inlet and bypass channels. Bypass is subtracted because it diverts water upstream of the basin, following the data release definition. At reading j, the net inlet rate p_j is converted from L/s to m³/h. The mean of adjacent readings defines the piecewise-constant six-minute rate q_j:

$$p_j=3.6\left(q_{\text{small},j}+q_{\text{large},j}-q_{\text{bypass},j}\right),$$
$$q_j=\frac{p_j+p_{j+1}}{2} \quad (1)$$

Adjacent-reading means preserve trapezoidal integration. Four negative intervals in 2014_2_15 total −0.934244 m³; clipping them for modeling increases record volume from 47.482040 to 48.416283 m³ without changing B or either reporting envelope at any tested duration. Source files remain unchanged (Supplementary Section S8). All bounds concern the reconstructed six-minute signal.

A threshold episode contains flow above 10 m³/h and is separated from another by at least six hours at or below that threshold. This identifies 28 episodes in 21 records; one record never exceeds the threshold. Fixed-block calculations use all 22 complete records, and the episode-summary analysis also preserves their full water volume and continuous storage.

Observed input discrepancy and hydraulic comparison

Blocks contain n_b native intervals of length δ = 0.1 h. Their durations Δ_b are 30, 60, 120 or 240 min, except for a shorter final block. The average $\overline{q}_b$ conserves the nonnegative volume V_b in every block. Define the cumulative residual D and its range B by

$$\overline{q}_b=V_b/\Delta_b, \qquad D(t)=\int_0^t [q(s)-\overline{q}(s)]\,ds,$$
$$B=\max_t D(t)-\min_t D(t). \quad (2)$$

Each block boundary has D = 0. The range B measures within-block timing discrepancy in storage units, independently of hydraulic parameters. For the scalar comparison, storage follows a common drainage law $f(t,S)$, nondecreasing in S, with the same initial state in both runs. At zero storage, drainage is limited by water availability. Assuming a well-posed reflected solution, define the peak requirement C_q over the common observation horizon T:

$$\dot{S}=q-f(t,S), \quad S>0, \qquad \dot{S}=\max\{0,q-f(t,0)\}, \quad S=0, \qquad C_q=\max_{0\le t\le T} S_q(t) \quad (3)$$

The peak-storage comparison is

$$|C_q-C_{\overline{q}}|\le B \quad (4)$$

Equation 4 uses the contraction structure of reflected storage (Kruk et al., 2007; Le Boudec and Thiran, 2001). Supplementary Section S1 proves it for monotone drainage, and Section S2 gives the passive-linear total-storage extension. The nonlinear layered model is evaluated numerically.

Error envelopes from retained block information

Suppose the report retains V_b and an interval-rate ceiling Q_b for each block. Among all compatible nonnegative six-minute profiles, the largest one-sided cumulative residual in block b is

$$m_b=\max_{k=0,\dots,n_b}\left(\min(V_b,Q_b k\delta)-\frac{kV_b}{n_b}\right) \quad (5)$$

An early pulse attains the positive extreme, and its time reversal attains the negative extreme. Ordering the m_b values from largest to smallest gives the exact global envelope

$$B\le E_{V,Q}=m_{(1)}+m_{(2)}\le E_V,$$
$$m_b^V=V_b(1-1/n_b) \quad (6)$$

Here Ev sums the two largest volume-only values m_b^V; a missing second block contributes zero. Opposite extrema can occur in different blocks, while one block has residual range at most m_b. Supplementary Section S3 proves the bounds and their attainment by compatible inflows.

Without ordering information, even block minimum and maximum do not determine B: (0,2,0,2) and (0,0,2,2) share volume, minimum and maximum but have different residual ranges. Continuous-profile bounds are given in Supplementary Section S3.

A compact alternative is to retain the maximum and minimum cumulative residual within each block. If $d_b(\tau)=\int_0^\tau q\,(t_b+s)\,ds-\overline{q}_b\tau$, report $u_b=\max d_b$ and $l_b=-\min d_b$. These two volume-valued fields recover the exact residual range:

$$B=\max_b u_b+\max_b l_b,$$
$$B\le\tilde{B}<B+2r \quad (7)$$

The second statement applies when each nonnegative field is rounded upward to a grid of spacing r. The extrema recover B, the error bound in Equation 4, without reconstructing the inlet trace (Supplementary Section S4). The

Table 1. Complete monitoring records and reconstructed nonnegative inlets

Record ID	Readings	Duration (h)	Volume (m³)	Peak (m³/h)	Episodes
2013_9_18	931	93.0	1638.680	132.915	2
2013_11_28	861	86.0	343.291	80.558	2
2014_1_5	146	14.5	8.660	8.087	0
2014_2_15*	598	59.7	48.416	56.263	1
2014_2_25	42	4.1	9.498	17.792	1
2014_4_19	705	70.4	52.412	49.727	1
2014_4_26	710	70.9	56.699	56.186	1
2014_5_22	1120	111.9	805.923	310.617	1
2014_7_12	2376	237.5	4281.834	236.464	3
2014_7_17	370	36.9	691.208	127.830	1
2014_11_24	576	57.5	583.903	148.895	1
2014_12_6	985	98.4	519.254	97.183	1
2015_4_2	1280	127.9	222.263	117.314	1
2015_4_24	1149	114.8	674.359	142.002	4
2015_5_5	333	33.2	74.261	36.535	1
2015_5_13	1530	152.9	2458.728	242.359	1
2015_6_9	391	39.0	134.210	50.641	1
2015_8_5	1111	111.0	2121.074	112.128	1
2015_9_2	625	62.4	319.783	82.327	1
2016_6_17	609	60.8	528.270	100.832	1
2016_6_28	467	46.6	77.786	25.814	1
2016_8_12	286	28.5	129.672	48.444	1

Note: Four negative intervals are clipped for modeling only. Episodes use the 10 m³/h and six-hour separation criteria; zero means that the threshold was never exceeded.

worst-case envelopes E_v and $E_{v,Q}$ instead bound all six-minute inputs compatible with their respective reported fields.

The producer computes the extrema from fine inflow before publishing the averaged series. For one partition, two global values $u_* = \max_b u_b$ and $l_* = \max_b l_b$ recover $B = u_* + l_*$. The designer uses the reported fields to calculate the averaged requirement and storage bound; per-block extrema retain additional local information.

The scalar model starts empty at fixed outflow F=18, 54 or 180 m³/h, equivalent to $K_{sat}A/100$ for 10, 30 or 100 mm/h over 1,800 m². These dimensional reference rates are held constant across records. Averaging cannot increase required storage in this model because it linearly interpolates cumulative net inflow at block boundaries (Supplementary Section S6).

Write C_f=C_q and C_a=$C_{\overline{q}}$ for the fine- and averaged-input requirements. Relative underestimation is $100(C_f\text{-}C_a)/C_f$. Here, "storage loss" denotes the reduction in calculated required storage caused by averaging, rather than a physical loss of water. The same usage applies to reductions in simulated surface peaks. Relative summaries use C_f>1 m³ and report medians with interquartile ranges; groups of three use the full range. All absolute requirements remain in the archive. Illustrations use the same fixed outflow rate of 54 m³/h. The main partition starts at the first timestamp. Four tested block origins are summarized in the results. Supplementary Section S16 reports the detailed sensitivity and the adapted flow-irregularity calculation (Baker et al., 2004).

Storage estimates and a chosen error tolerance

Let E denote any one of the available error bounds: the observed residual range B, the volume-and-peak envelope $E_{V,Q}$, or the volume-only envelope E_V. Equation 4 gives a conservative estimate of required storage, $C^+ = C_a + E$. Under the stated hydraulic assumptions, a prescribed capacity C_d is sufficient if $C^+ \le C_d$. In that case,

$$C_f \le C^+ = C_a + E, \qquad C_a + E \le C_d \tag{8}$$

We report the median ratio C^+/C_f to measure the excess storage associated with each inflow summary. This is a deterministic margin for temporal aggregation of the reconstructed inlet, separate from uncertainty in parameters or future forcing. For constant outflow, $C_a \le C_f \le C_a + E$. If $C_a > 0$, the reported bound gives the following sufficient check for a relative-underestimation tolerance $0<\varepsilon<1$:

$$\frac{C_f - C_a}{C_f} \le \frac{E}{C_a + E}, \qquad \frac{E}{C_a + E} \le \varepsilon \quad \Leftrightarrow \quad E \le \frac{\varepsilon}{1-\varepsilon} C_a \tag{9}$$

We use 25% as an illustrative design tolerance, not a regulatory threshold. At that value, the operational criterion is $E \le C_a/3$. The producer can use this criterion to select a reporting interval for a declared outflow rate, and the designer can repeat it from the averaged series and reported bound. The separate retrospective test $E \le 0.25_f$ requires the fine-input result and is retained for comparison. Failure of either test means that the retained information does not establish the tolerance; it does not establish that the actual error exceeds 25%. Supplementary Section S14 gives the derivation, zero-storage cases and the different criterion for a two-sided relative error. Layered-model ratios are evaluated from simulated surface peaks; they are numerical tests of the margin, not prospective guarantees for that model.

Required storage from maximum volume by duration

For a nonnegative inlet over $[0,T]$, empty initial storage and constant outflow F, define $M(\tau)$ as the maximum volume in any contiguous interval of duration τ. The required storage is

$$M(\tau) = \max_{0 \le s \le T-\tau} \int_s^{s+\tau} q(t)\, dt, \qquad C(F) = \max_{0 \le \tau \le T} \{M(\tau) - F\tau\} \tag{10}$$

Here $M(0)=0$ includes zero storage. Grouping the maximum cumulative net-input increment by interval duration gives Equation 10, the finite-record constant-outflow form of the classical backlog/envelope construction (Le Boudec and Thiran, 2001). For the piecewise-constant signal, six-minute boundary times suffice. Rain-envelope sizing similarly compares accumulated inflow with assumed outflow, with an additional approximation when a depth-dependent outlet is replaced by a constant rate (Santos et al., 2021). Supplementary Section S15 gives the derivation.

The sparse duration set is 6, 12, 30, 60, 120, 240, 360, 720 and 1440 min, omitting durations longer than the record. These values provide compact coverage from the six-minute sampling interval to daily accumulation, including the tested averaging durations. They are an example reporting set rather than an optimized universal choice. Maximizing zero and $M(\tau)$-$F\tau$ over this subset gives a lower bound. Accumulation beyond 24 h calls for longer durations within the observation horizon and closer spacing around periods controlling storage. The complete-curve implementation was checked against direct storage routing for all 22 records and three outflow rates (Supplementary Section S15).

For the same nonnegative reconstructed inlet, an initially empty store and a constant outflow rate F over $[0,T]$, let C_D be the maximum of zero and $M(\tau)$-$F\tau$ over any retained duration set D. If C_a uses volume-preserving block averages and B is their cumulative-residual range, then

$$C_- = \max\{C_a, C_D\} \le C_f \le C_+ = C_a + B \tag{11}$$

The lower endpoint combines the averaging result in Supplementary Section S6 with the restricted maximization in Equation 10; Equation 4 gives the upper endpoint. The interval applies to the specified inlet and constant-outflow model. For nine durations, $C_D = C_9$: at most nine maximum-volume values plus two global residual extrema are added to the averaged hydrograph. Record length, block definitions and duration labels must also be retained. These same fields can be used at different constant outflow rates for the declared partition. Rounding duration maxima downward and residual extrema upward preserves the bounds when published block volumes remain consistent (Supplementary Section S15).

Containment was tested in 264 record–outflow–block combinations. Endpoint ratios use $C_f > 1$ m³ and $C > 0$. Diagnostic extensions add 48 and 96 h, the terminal duration T, or both, omitting values beyond T. The terminal value $M(T)=V$ is already recoverable from block volumes.

Episode-summary comparison

To evaluate event volume and peak fields, we partitioned the 21 threshold-positive records into 28 episode blocks, splitting each separating quiet gap at its midpoint. Leading and trailing flow remains in the first and last block; the threshold-free record is retained as one background block. Each block contributes its duration, volume and six-minute peak to Equations 5–6. Averaged inputs and bounds are routed over the complete original record without resetting storage between episodes. This is an explicit inflow-based delineation, rather than the rainfall-defined storm eligibility used by monitoring protocols. Supplementary Section S17 describes the delineation, identifies the archived episode boundaries and gives a narrower core-episode sensitivity.

Layered bioretention simulations

Simulations used the U.S. Environmental Protection Agency Storm Water Management Model, engine 5.2.4, through swmm-toolkit 0.17.0 and PySWMM 2.1.0 (McDonnell et al., 2020; Rossman and Simon, 2022). The bioretention implementation represents surface, soil and gravel water with state-dependent fluxes (Rossman and Huber, 2016). Each nonnegative inlet was encoded as an equivalent six-minute rainfall intensity over a single 1,800 m² subcatchment fully occupied by the bioretention unit. This nominal biofilter area is reported for Wicks Reserve (Browne et al., 2024). The encoding imposes the measured inlet shape; it is not a reconstruction of observed rainfall or upstream runoff generation.

The three prescribed parameter configurations in Table 2 span restricted infiltration and drainage (P1), an intermediate regime (P2), and more rapid transmission through the soil and drainage layers (P3). P1 also has a shallower soil layer. Conductivity, soil thickness, exfiltration and drain coefficient vary together, so their responses compare combined storage and drainage regimes rather than isolated conductivity effects. Soil porosity, field capacity and wilting point are 0.45, 0.15 and 0.08; conductivity slope is 30 and suction head 50 mm. Gravel thickness is 300 mm and void ratio 0.75. The drain exponent is 0.5, its offset is zero, and baseline runs start with zero initial saturation above the wilting point. The surface vegetation fraction is zero, Manning roughness is 0.1 and slope is 1%. Evaporation is zero. These prescribed configurations are not calibrated Wicks models.

The field-validated Wicks model uses a 900 m² ponding area and 1.800 m² filter area, a bulk filter conductivity of 1.800 mm/h and an effective outlet coefficient of 0.002 (Bonneau, Lipeme Kouyi, et al., 2021). Its stepwise saturation-profile representation and outlet relation differ from SWMM's soil/gravel states and drain law. The published 0.8 m filter depth also includes drainage material. Copying these fitted coefficients would therefore not transfer the field calibration. Here, the uniform 1.800 m² model surface and prescribed hydraulics isolate temporal-information effects. Reported depths are equivalent model depths, rather than predictions of observed ponding at Wicks.

For an antecedent-wetness sensitivity, P2 was rerun with soil water at field capacity, θ_0=0.15, for all 22 fine inputs and their one-hour and four-hour averages. SWMM's initial saturation setting is 100 (0.15–0.08)/(0.45–0.08) = 18.919% and also initializes the gravel to 56.757 mm of water. These 66 runs therefore change soil and gravel wetness together; all other input settings remain unchanged (Supplementary Section S18).

Runoff and routing steps are 30 s. Every fine–averaged pair shares parameters, initialization and simulation horizon. Full-precision surface depth, soil moisture and gravel depth are read through the application programming interface at each 30 s step, including the terminal state. Total storage in m³ is $A[h_s+\theta\, d_s+h_g\phi_g]$, where A is model area, h_s surface-water depth, θ volumetric soil water content, d_s soil thickness, h_g gravel-water depth,

Table 2. Prescribed layered-model configurations and corresponding scalar reference rates

Set	Conductivity (mm/h)	Soil depth (mm)	Exfiltration (mm/h)	Drain coefficient	Outflow F (m³/h)
P1	10	500	2	0.5	18
P2	30	800	5	1.0	54
P3	100	800	20	5.0	180

Note: The drain law is $q=Ch^{0.5}$, with q in mm/h and h in mm; coefficient units are $mm^{0.5}/h$. All paired simulations share their configuration.

and ϕg=0.75/(1+0.75) gravel porosity. Depths are in mm and area in m². Total storage includes initial soil and gravel water. The main surface berm is 10.000 mm to prevent overflow from clipping either trajectory. A separate 300 mm berm test evaluates surface overflow under the same forcing and parameters; this is a prescribed depth sensitivity within the range discussed in design guidance (U.S. Environmental Protection Agency, 2021). The report-rounding diagnostic and its nine apparent bound exceedances are documented in Supplementary Section S10.

The monitored-forcing comparison comprises 22 records × three configurations × five inlet resolutions, or 330 runs and 264 fine–averaged pairs. Peak and maximum absolute trajectory differences are evaluated separately for total and surface storage. Surface-loss percentages use fine-input ponding above 1 m³; a 25 m³ threshold tests denominator sensitivity. Fine-input scalar requirements are compared with surface peaks in absolute units and after dividing both by the corresponding record volume. The raw and volume-normalized correlations use the same records with fine-input surface peaks above 1 m³ in P1 and P2; P3 has only three qualifying records and is reported descriptively. Each loss correlation is computed separately by configuration and averaging duration, with one observation per record. No pooled coefficient or significance test is used. Inputs, reports, full-precision traces and executable analysis scripts are archived together.

Controlled inputs with identical summaries

To test whether exact residual-extrema reporting identifies required storage, we constructed two scalar inputs over four segments of duration τ: a central pulse $(0,2F,0)$ and separated pulses $(2F,0,0,2F)$. With a native interval dividing τ, both have the same volume, peak, rate histogram and residual extrema. Starting empty under the same constant outflow rate F, their storage requirements are $2F\tau$ and $F\tau$, although both have $B=2F\tau$. Supplementary Section S12 proves this construction and the resulting lower bound on any estimate of required storage based only on their common summaries.

The layered experiment tests all six permutations of (0,0,Q,Q) with one-hour segments, Q = 108 or 216 m³/h, and eight subsequent hours of zero inflow under P2. The central and separated pair was specified before execution; the remaining orders provide controls. Including each common four-hour average gives 14 runs at 30 s, with six repeats at 15 s. The protocol, hashes and complete outcomes are archived (Supplementary Section S13).

RESULTS

Storage loss after averaging

Fine-input storage requirements above 1 m³ occurred in 20, 13 and three records at fixed outflow rates of 18, 54 and 180 m³/h, respectively. At 18 m³/h, median loss was 3.4% at one hour and 12.8% at four hours. At 54 m³/h, it rose from 12.5% to 89.2% over the same durations (Table 3). Eleven of the 13 qualifying records exceeded a 25% loss at four hours. For the three records qualifying at 180 m³/h, median loss was already 80.3% at 30 min and reached 100% at one hour.

A 100% loss means that every averaged block in the relevant record stayed below the prescribed outflow rate, while a native pulse required storage. This threshold behavior explains the high-outflow result and its small denominator. Each outflow rate is applied unchanged to every record. The difference between the 18 and 54 m³/h results therefore reflects the drainage regime, rather than an event-specific choice of outflow.

The May and July records illustrate storage loss at the same 54 m³/h outflow (Figure 1): concentrated inflow accumulates, whereas averaging shifts some inflow into periods when drainage has already reduced storage.

For P2, 12 records had fine-input surface peaks above 1 m³. Their median surface losses were 6.0%, 20.4%, 39.3% and 100% at 30, 60, 120 and 240 min; three, five, seven and eleven records, respectively, exceeded 25% loss. Raising the fine-peak threshold to 25 m³ left eight records and a four-hour median loss of 71.2%. Figure 2 shows the distribution and the paired depth comparison. The largest P2 fine-input surface peak among monitoring records, in 2014_5_22, corresponds to 113.168 mm; the one-hour and four-hour inputs yield 105.289 and 54.152 mm. The four-hour decrease is 59.016 mm, or 106.228 m³.

Three 30-min pairs slightly increased peak surface water after averaging: 2014_4_26 in P1, 2014_7_17 in P1 and 2015_5_13 in P2 (Supplementary Section S9). The layered model therefore permits departures from the scalar model's one-sided peak reduction. Across the monitored-forcing configurations and durations, total-storage

Table 3. Loss of required storage after temporal averaging (%): median [interquartile range], except F = 180 m³/h, for which brackets give the full range

F (m³/h)	n	30 min	60 min	120 min	240 min	>25% at 240 min
18	20	1.3 [0.4–6.4]	3.4 [0.5–13.8]	7.9 [1.9–62.7]	12.8 [6.4–100.0]	7/20
54	13	5.0 [3.9–8.5]	12.5 [8.1–36.1]	34.7 [15.9–100.0]	89.2 [47.8–100.0]	11/13
180	3	80.3 [32.9–100.0]	100.0 [32.9–100.0]	100.0 [100.0–100.0]	100.0 [100.0–100.0]	3/3

Note: Only records with fine-input required storage above 1 m³ are included; the same records are used at all four durations within each fixed outflow rate. A 100% loss means the averaged input requires no storage. Quartiles use linear interpolation of the ordered sample; the three records at F = 180 m³/h are described by their full range.

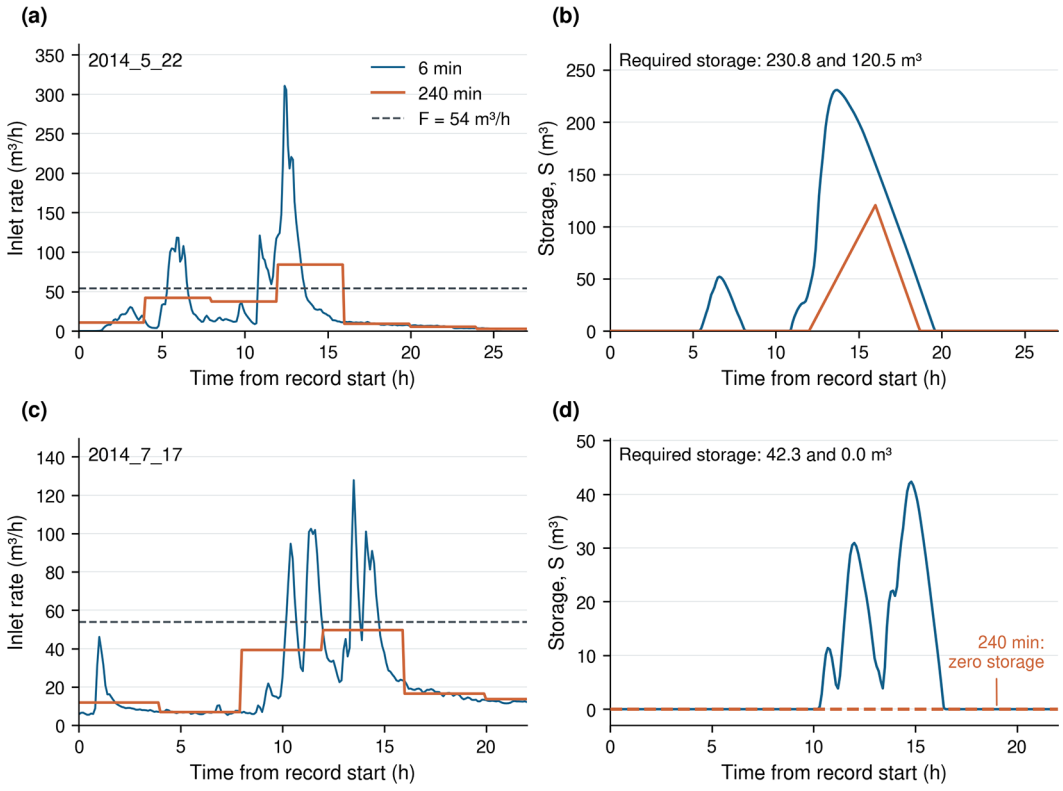

Figure 1. Inflow and scalar storage at F = 54 m³/h for (a,b) 2014_5_22 and (c,d) 2014_7_17. Blue uses six-minute inflow; orange uses volume-preserving four-hour averages. Dashed lines in (a,c) mark F. The first 27 and 22 h are shown; all storage maxima use complete records. Fine and averaged requirements are 230.849 and 120.466 m³ in May (B = 204.215 m³), and 42.316 and 0 m³ in July (B = 81.240 m³). The dashed orange trajectory in (d) is zero; the negative axis margin makes it visible

peaks changed by at most 7.6%, compared with 1.9% within P2. These percentages include the initial soil water, so they describe total modeled storage rather than the fraction of event water retained.

With a 300 mm berm, two records produced more than 1 m³ of surface overflow, both in P1: 2014_7_12 and 2015_5_13. Fine-input overflow volumes were 436.45 and 362.09 m³. Every averaged version of these two cases also overflowed; averaging concealed neither exceedance. The larger differences in the monitored-forcing experiment concern the ponding depth required below the berm, while the overflow outcome also depends on the chosen capacity threshold.

In the wet-initialization P2 comparison, the same 12 baseline records had median one-hour and four-hour surface losses of 19.8% and 99.9%, compared with 20.4% and 100% when initialized at the wilting point. Counts above 25% loss remained 5/12 and 11/12. Fine-input surface peaks increased by a median 2.280 m³; the maximum increase was 10.202 m³. One additional record crossed the 1 m³ selection threshold. All 44 wet-initialization pairs remained

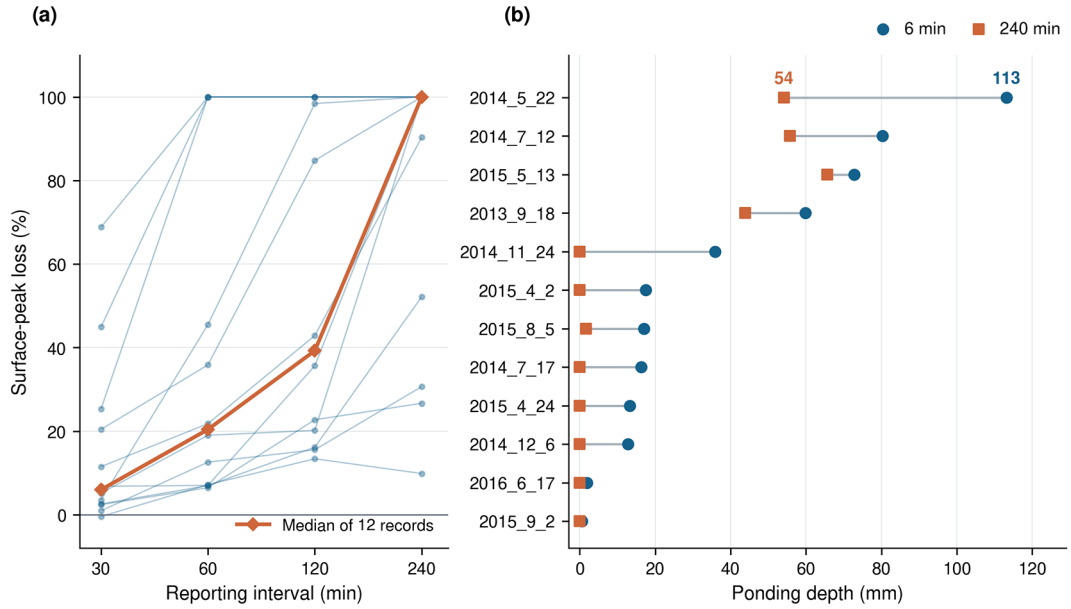

Figure 2. Simulated P2 surface ponding for 12 records with fine-input surface storage >1 m³. (a) Relative peak loss after averaging, with individual records as thin lines and medians as a thick line; negative values mean increased ponding. (b) Fine and four-hour peaks as equivalent depths over the model's 1,800 m² area, ordered by fine-input depth. For 2014_5_22, fine, one-hour and four-hour peaks are 113.168, 105.289 and 54.152 mm. P2 has conductivity 30 mm/h and a high berm to avoid truncating storage

below B for sampled total- and surface-storage differences (Supplementary Section S18).

Storage margins from retained inflow fields

Across the 22 records, the median residual range B divided by record volume increased from 2.4% at 30 min to 5.0%, 9.5% and 16.1% at 60, 120 and 240 min (Figure 3). The four-hour absolute range was 3.519–204.215 m³, with a median of 47.245 m³. Four tested block origins changed B by median factors of 1.52–1.62 across durations, with a maximum factor of 3.96. The partition therefore forms part of the reporting specification. Detailed origin and flow-irregularity results are in Supplementary Section S16.

Adding block peaks to block volumes reduced the worst-case envelope by 11.9–81.9%, with a median reduction of 51.2% across 88 record–duration combinations. Recording cumulative-residual extrema reduced the remaining envelope by 25.5–76.9%, with a median of 49.4%. Every observed *B* lay below the volume-and-peak envelope. Figure 4 identifies all records in the four-hour hierarchy; the complete numerical table is in Supplementary Section S8. Thus a peak provides useful information, while the ordering of water within each block still accounts for a substantial part of the remaining uncertainty.

Every scalar requirement was covered by C_a + *E*. At 54 m³/h and four hours, its median ratio to fine-input storage was 6.50 with volumes, 3.34 with peaks and 1.75 with extrema (Table 4). These summaries preserve the same volume but require different margins for unresolved timing.

Adding *B* to the averaged P2 surface peak also covered every fine-input surface peak in the tested records. Among the 12 records above 1 m³, its median ratio increased from 1.18 at 30 min to 2.23 at four hours. The same ratios increased further when peaks or volumes provided only a worst-case envelope (Table 4). The ratios measure the excess associated with this conservative correction.

Table 5 compares retrospective and operational tolerance checks. At 30 min and 54 m³/h, the retrospective criterion established a loss of at most 25% for 0, 4 and 8 of 13 records using volumes, peaks and extrema; the operational criterion did so for 0, 7 and 9. Every successful check agreed with the calculated loss. With extrema, five records passed at one hour, one at two hours and none at four hours.

Margins for episode summaries

The complete episode blocks span 4.1–162.8 h and retain all recorded water; 12.65% of total volume lies outside the first-to-last

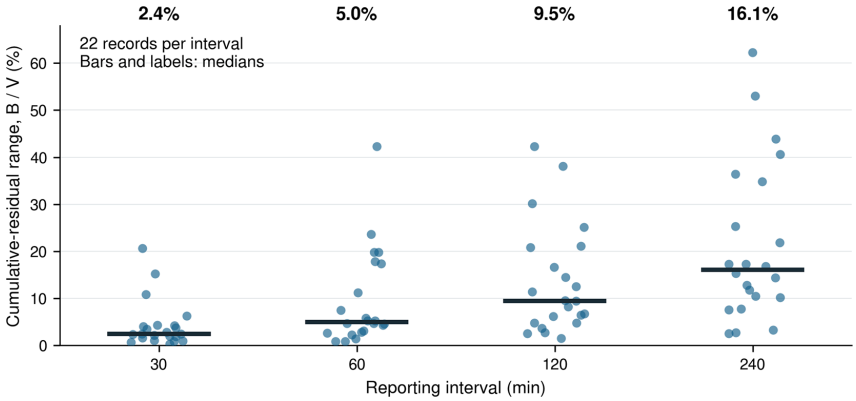

Figure 3. Residual range B divided by record volume V for all 22 monitoring records. Each point is one record; horizontal bars show medians of 2.4, 5.0, 9.5 and 16.1% at 30, 60, 120 and 240 min. Horizontal jitter separates points. Blocks start at the first timestamp; alternative origins are summarized in Supplementary Section S16, Table S10

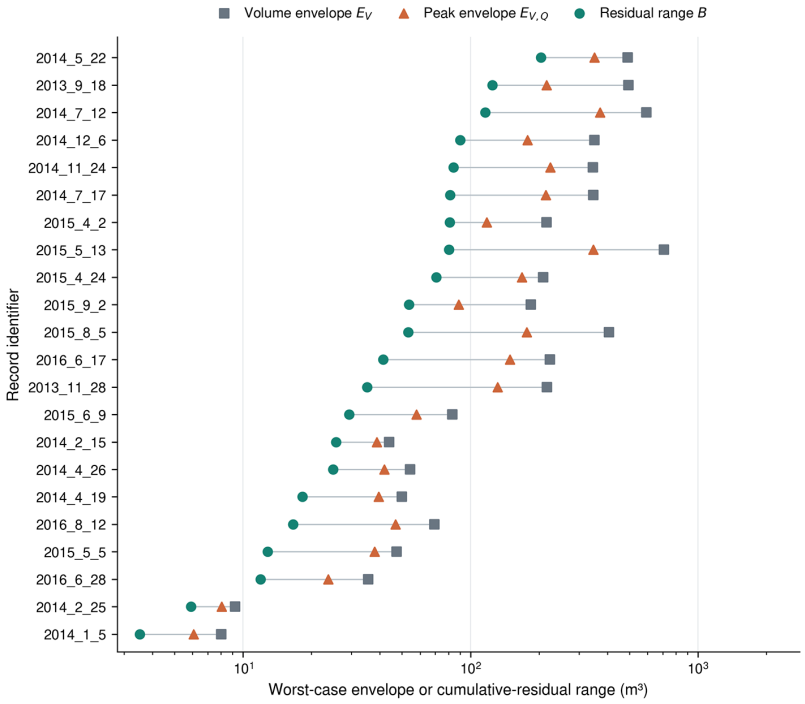

Figure 4. Four-hour reporting bounds for all 22 records, ordered by descending B. Lines join the volume-only envelope E_v, volume-and-peak envelope $E_{V,Q}$ and observed residual range B. The horizontal axis is logarithmic. Record identifiers follow the source filenames. The extrema recover B exactly for the declared partition

threshold-exceedance cores. Their largest mean inflow is 20.680 m³/h, so averaging by episode gives zero required storage at 54 and 180 m³/h. The resulting loss is a consequence of these long averaging periods. Nevertheless, the volume and peak bounds cover the fine-input requirement in all 66 complete-record comparisons. At 54 m³/h, adding peaks lowers the median upper/fine ratio only from 12.57 to 11.80, while residual extrema lower it to 5.42 (Table 6). This is larger than the four-hour extrema margin of 1.75 for the same records. Retaining event volume and peak therefore provides limited control of unresolved timing under this delineation.

Narrowing each episode to its first and last threshold exceedance retained 87.35% of total volume across all 22 records. For the same 24 initially empty episodes requiring more than 1 m³ at 18 m³/h, median averaging loss fell from 100% with complete episode blocks to 33.1% with these

Table 4. Conservative storage estimate divided by the fine-input requirement: median [interquartile range]. Scalar rows use constant outflow; P2 rows use SWMM surface-storage peaks

Model / outflow rate	Block (h)	n	Volumes + extrema	Volumes + peaks	Volumes only
Scalar, F = 18 m³/h	1	20	1.12 [1.07–1.37]	1.28 [1.15–2.24]	1.79 [1.56–3.10]
Scalar, F = 18 m³/h	4	20	1.35 [1.18–1.75]	1.91 [1.62–3.70]	2.58 [2.14–4.76]
Scalar, F = 54 m³/h	1	13	1.21 [1.13–1.31]	1.61 [1.41–2.12]	3.31 [2.41–4.30]
Scalar, F = 54 m³/h	4	13	1.75 [1.41–2.11]	3.34 [2.47–5.06]	6.50 [4.37–8.20]
SWMM, P2	1	12	1.32 [1.24–1.52]	2.13 [1.54–2.47]	4.51 [2.77–5.59]
SWMM, P2	4	12	2.23 [1.51–3.20]	4.80 [3.42–7.40]	7.78 [5.33–13.86]

Note: Estimates add B, $E_{V,Q}$ or E_V to the averaged requirement and divide by fine-input required storage. All denominators exceed 1 m³. Quartiles use linear interpolation. The guarantee is scalar; P2 ratios describe simulated surface peaks.

Table 5. Records meeting a bound-based tolerance check for at most 25% relative underestimation at F=54 m³/h. The benchmark group contains 13 records with C_f>1 m³

Block (min)	Retrospective V	Retrospective V,Q	Retrospective extrema	Operational V	Operational V,Q	Operational extrema
30	0/13	4/13	8/13	0/13	7/13	9/13
60	0/13	0/13	2/13	0/13	0/13	5/13
120	0/13	0/13	0/13	0/13	0/13	1/13
240	0/13	0/13	0/13	0/13	0/13	0/13

Note: The retrospective check is $C_a \leq 0.25C_f$; the operational check is $E \leq C_a/3$, $C_a > 0$ with. For volume-only, volume-and-peak, and residual-extrema summaries, E equals E_V, E_{VQ}, and B, respectively. The benchmark group is defined using fine-input results, whereas the operational check itself requires only the averaged requirement and the reported fields. Failure of a check does not establish that the actual underestimation exceeds 25%.

narrower cores; their fine-input maxima were unchanged. Thus the boundary convention changes the averaging error even when it preserves the storage-driving pulse. These separate episode diagnostics do not replace the complete-record comparison or assume that six quiet hours drain every store (Supplementary Section S17).

What the summaries determine

The constructive scalar pair has identical volume, peak, histogram and cumulative-residual extrema, yet the central pulse requires twice the storage of the separated pulses. Thus retaining the exact residual range B leaves required storage unidentified. Any deterministic estimate $\hat{C}$ based on these common summaries must incur an absolute error of at least B/4 for one member of the pair (Supplementary Section S12). This is a lower bound for the constructed pair, distinct from the upper error bound for averaging in Equation 4.

The controlled layered responses show the same information distinction (Figure S1). At Q=108 m³/h, central and separated pulses produced peak surface depths of 27.865 and 21.363 mm, a difference of 6.503 mm; the common average produced zero ponding. At Q=216 m³/h, the respective depths were 130.246 and 82.741 mm, compared with 70.902 mm for the common average. The primary contrast is therefore 47.506 mm, or 85.510 m³, despite identical reported volume, peak, histogram and residual extrema. The three placements of a continuous two-hour pulse gave identical peaks; the complete permutation results are in Table S7.

Controlled runs had absolute continuity errors below 0.005811%. Halving the step changed individual surface peaks by at most 0.022 mm and the contrasts by 0.020 mm. Total- and surface-storage trajectory differences stayed within B; maximum ratios were 1.000 and 0.853 (Table S8).

The nine-duration product alone underestimated required storage by a median 3.5% at F=18 m³/h and 7.3% at F=54 m³/h among the respective 20 and 13 records above 1 m³. Its largest loss was 44.3% at F=18 m³/h, where three critical durations exceeded 24 h.

Table 6. Conservative bounds from complete episode summaries, with storage continuous over the original record. Values are medians [interquartile range] of the upper bound divided by fine-input required storage

F (m³/h)	n	Volumes only	Volumes + peaks	Volumes + extrema
18	20	3.85 [2.68–6.29]	3.34 [2.58–6.10]	1.52 [1.29–3.63]
54	13	12.57 [9.44–27.96]	11.80 [8.93–25.58]	5.42 [4.34–7.16]

Note: The same C_f>1 m³ cohorts are used as in Tables 3–4. The partition retains 28 episode blocks and one background block across 22 records; no hydraulic reset is imposed. All three bounds include the averaged-input requirement. The three qualifying records at 180 m³/h are summarized in Supplementary Section S17; individual values are archived.

Combining this product with the averaged requirement and B enclosed C_f in every one of the 264 record–outflow–block combinations. Table 7 shows the selected-group endpoint ratios. At one hour, the median upper-to-lower ratio was 1.14 for F=18 m³/h and 1.29 for F=54 m³/h. The median lower endpoint was 98% and 95% of the fine-input requirement, respectively. The upper endpoint is the same conservative estimate used in Table 4; the duration maxima improve the information available below it.

Adding 48 and 96 h to the sparse duration set reduced its median loss at F=18 m³/h from 3.5% to 3.1% and its maximum from 44.3% to 10.9%. The three records with critical durations above 24 h improved, but the combined-interval medians in Table 7 were unchanged: the averaged requirement already supplied the stronger lower bound in two of those records. Adding only the terminal point $M(T)=V$ changed none of the 66 sparse estimates. Supplementary Section S15 reports the extension results and duration coverage.

The central and separated profiles have the same one-hour maximum volume, Q(1 h), but two-hour maxima of 2Q(1 h) and Q(1 h). At Q = 108 and F = 54 m³/h, these distinguish required storage of 108 and 54 m³ (Figure S1d). Residual extrema preserve their common B; duration maxima distinguish their requirements.

Scalar and layered-model comparison

The 330 main simulations driven by monitoring records completed with an absolute LID continuity error below 0.013%, calculated from full-precision water balances. The analysis includes the terminal state of every run (Supplementary Section S11). The largest total-storage and surface-storage trajectory differences were 0.871B and 0.904B, respectively. Every monitored-forcing pair remained within B for both sampled quantities.

For fine-input surface peaks above 1 m³, Spearman correlations between scalar required storage and SWMM surface peaks were 0.979 in P1 (n = 16) and 0.937 in P2 (n = 12). Dividing both quantities by record volume gave 0.759 and 0.853, respectively. Absolute storage volumes therefore agreed more closely in rank than stored fractions, particularly in P1. These comparisons describe the prescribed configurations; both normalized quantities share the volume denominator. P3 had three qualifying records and was excluded from correlation reporting (Figure 5).

For losses after averaging, Pearson correlations were calculated separately for each configuration and duration, with one observation per record. They ranged from 0.166–0.593 in P1 (n = 16 per duration) and 0.554–0.855 in P2 (n = 12 per duration). Each coefficient describes a single prescribed configuration and reporting interval; no significance tests were used.

DISCUSSION

What the summaries preserve

The analysis links inflow summaries to storage decisions using established reflected-storage and envelope theory (Kruk et al., 2007; Le Boudec and Thiran, 2001). For a declared partition, volumes give a worst-case error bound, peaks narrow it, and two residual extrema recover B. Duration maxima add a lower bound through Equation 10, which is combined with the averaging bound in Equation 11. The complete curve determines required storage across constant outflow rates. The distinction is quantitative: the summary controls both the conservative margin and whether the available storage can be classified as sufficient or insufficient.

The controlled pair demonstrates why an exact error bound alone does not determine storage.

Table 7. Combined interval using nine duration maxima and the observed residual range. Each entry is the median of the indicated record-level ratio

F (m³/h)	Block (h)	Records	C_+/C_-	C_-/C_f	C_+/C_f
18	1	20	1.14	0.98	1.12
18	4	20	1.40	0.98	1.35
54	1	13	1.29	0.95	1.21
54	4	13	1.82	0.93	1.75

Note: C=max(Ca,C_9) and C_+=C_a+B. Groups require C_f>1 m³; their lower endpoints are positive. The endpoint ratio measures multiplicative interval width, not relative error or a confidence level. Medians of ratios are calculated separately and need not equal ratios of medians.

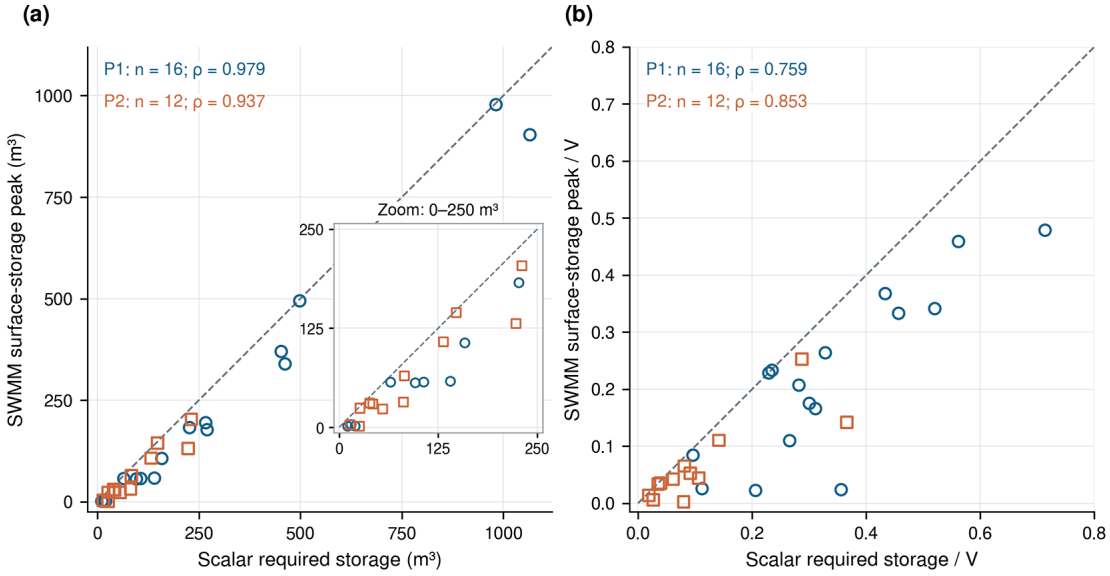

Figure 5. Scalar required storage and SWMM surface peaks for P1 (n = 16) and P2 (n = 12), using the same 28 record–configuration combinations from 16 records in both panels. Selection requires fine-input surface storage >1 m³. (a) Absolute volumes; the inset enlarges 0–250 m³. (b) Both values divided by the corresponding record volume V. Dashed lines mark equality. Scalar rates are 18 and 54 m³/h; SWMM fluxes depend on model state. P3 has only three qualifying records and is omitted. The correlations are descriptive; normalized values share a denominator

Its common summaries allow a 47.51 mm difference in P2 ponding at the higher loading. A two-hour volume maximum distinguishes the pair where a one-hour maximum does not. The BMP Database already requests maximum one-hour rainfall intensity (Wright Water Engineers, Inc. & Geosyntec Consultants, 2019); the analogous inflow field is *M*(1 h). Several inflow durations extend that reporting idea without equating rainfall and inflow.

Engineering interpretation and comparison with published work

Published temporal-resolution tests measure different hydraulic outcomes. Averaging radar rainfall from one minute to 5–10 min produced differences below 0.05 m in maximum sewer depth and shifted peak-depth timing by up to 10 min in one event (Bruni et al., 2015). Across seven catchments, changing rainfall and calibration-flow resolution from 24 to 12 h reduced mean absolute hourly peak-flow error from 27% to 21% (Tudaji et al., 2025a). Those experiments change rainfall forcing or calibration resolution. Here, each pair shares its measured inlet volume and hydraulic parameters, and the outcome is required storage. The reduction from 113 to 54 mm describes equivalent surface demand in the prescribed P2 model. Its size cannot be compared directly with rainfall-model errors or treated as an observed Wicks ponding depth.

This dependence on response and timescale is consistent with characteristic-timescale analysis (Castro et al., 2025).

Surface storage and subsurface fluxes serve different design functions (U.S. Environmental Protection Agency, 2021). Comparisons of two bioretention models with observations found that agreement in event volumes can differ from agreement in drainage-hydrograph shape (Lisenbee et al., 2022). Our results likewise separate water accounting from the surface peak, although they concern an input-representation experiment. Computational sizing tools convert rainfall information into tank and infiltration-trench dimensions (Białek and Musz-Pomorska, 2025), and the rain-envelope method makes an explicit outflow assumption (Santos et al., 2021). The present analysis quantifies the margin associated specifically with inlet reporting, alongside those other design assumptions.

The direction of temporal-loading effects depends on the transformation. Conventional design profiles produced larger detention requirements than frontal profiles in a previous comparison (Burns et al., 2026), while three of our averaged inputs slightly increased ponding. This agrees with published concerns about simplifying design assumptions (Sambito et al., 2026). An 80-storm field-validation comparison addresses observed hydraulic performance beyond the scope of the prescribed simulations used here (Wang et al., 2019).

The 2.4% median B/V at 30 min quantifies temporal aggregation relative to the reconstructed inlet, not instrument uncertainty. The Sigma 950 manual specifies velocity accuracy of ±2% of reading and depth accuracy of ±0.16% of full scale plus ±1.5% of reading at constant temperature (Hach Company, 2009). These component specifications do not give a 2% discharge uncertainty. Wetted area, field calibration and subtraction of bypass also affect reconstructed inflow, and their per-record uncertainties are unavailable. A crossover interval at which averaging error exceeds measurement error therefore cannot be determined from this release.

Volume normalization reduced scalar–SWMM rank agreement in P1 and P2, showing that record magnitude contributes to the raw correlations. Because both normalized quantities share the record-volume denominator, these associations describe this set of prescribed simulations rather than independently tested predictions. The dimensional rate $F=K_{sat}A/1000$ remains distinct from state-dependent layered drainage.

Choosing inflow fields for a storage decision

The monitoring team computes B from the fine record before publishing the averaged series. A database can calculate the block mean, subtract its cumulative linear trajectory from cumulative inflow, and retain the two extrema. A logger can perform the same calculation when a block closes, buffering up to 40 six-minute values for the longest tested block. This takes one linear pass through the block plus its buffer, whereas a peak alone needs only a running maximum. Duration maxima require a separate calculation across the record. Supplementary Section S4 gives the algorithmic details.

The designer uses the averaged hydrograph and reported fields to calculate C_a and test $C_a+E\leq C_d$ without the fine hydrograph. The producer can use the same check, or the chosen relative tolerance, to select a reporting interval. Keeping the original measurements permits later refinement and other hydraulic analyses. TAPE's five-minute or shorter logging requirement concerns acquisition and remains separate from this summary calculation (Howie and Milesi, 2026).

Table 8 compares the decisions supported by each product. For available storage $C_d \geq C_+$ is sufficient under constant outflow, whereas $C_d<C$ is insufficient. A value between the endpoints remains unresolved by the summaries. This three-way decision avoids treating a failed upper-bound check as proof of inadequate storage.

For record 2014_5_22, four-hour summaries at F = 54 m³/h give C_a = 120.466 m³ and B = 204.215 m³. Combining the nine-duration estimate with the averaged requirement and residual bound gives [206.053, 324.681] m³, with endpoints rounded outward from full-precision calculations. Available capacities of 325 and 200 m³ are therefore sufficient and insufficient, respectively; 250 m³ remains unresolved from these summaries. The decisions concern the reconstructed 111.9 h record with empty initialization and constant outflow. The 25% averaging-error check fails because $B > C_a/3$, although the capacity check succeeds at 325 m³.

The selected tolerance can guide interval choice. At 54 m³/h, 30 min with extrema

Table 8. Reporting fields, guarantees and design decisions under empty initialization and constant outflow. Every row assumes known record and duration definitions

Retained fields	Guarantee	Supported decision	Observed margin
Block volumes	$C_a \le C_f \le C_a + E_V$	Sufficient storage if $C_d \ge C_a + E_V$	Median upper/fine ratio 6.50
Block volumes and peaks	$C_a \le C_f \le C_a + E_{V,Q}$	Same sizing check with a narrower envelope	Median upper/fine ratio 3.34
Block volumes and residual extrema	$C_a \le C_f \le C_a + B$	Sizing; at most 25% underestimation if $B \le C_a/3$ and $C_a > 0$	Median upper/fine ratio 1.75
Block volumes, residual extrema and nine duration maxima	$C_- \le C_f \le C_+$	Sufficient, insufficient or unresolved storage	Median upper/lower ratio 1.82
Complete six-minute duration–volume curve	Exact $C(F)$ through Equation 10	Identify required storage at any constant F	No approximation from duration sampling

Note: The first four numerical margins use the same 13 records with $C_f > 1$ m³ at F=54 m³/h and four-hour blocks; they are observed medians, not universal factors. Sparse duration maxima alone supply only a lower estimate. The guarantees in this table apply to the scalar constant-outflow model.

established the 25% bound for nine of 13 records; four did not pass. A separate capacity decision may still succeed through the combined interval even when the relative-error criterion fails.

Duration coverage matters separately from the block interval. The sparse set must include accumulation periods relevant to the outflow regime; adding a terminal volume does not necessarily characterize concentrated inflow within a long record. The global extrema apply only to their declared averaging partition. Block origin must therefore accompany each published summary.

The guarantees concern the reconstructed inlet and stated initial conditions. The prescribed SWMM configurations test loading and drainage regimes, with dry and wetter P2 initialization. The high berm exposes surface demand, while the 300 mm test distinguishes reduced calculated storage demand from actual overflow. Agreement with B in these layered runs remains numerical evidence for those cases.

CONCLUSIONS

For the 13 records requiring more than 1 m³ at a constant outflow of 54 m³/h, four-hour averaging underestimated required storage by a median 89.2%, with underestimation above 25% in 11 records. In the prescribed layered P2 model, the largest surface requirement decreased from 113 to 54 mm. Temporal averaging therefore changed the modeled surface-design requirement despite preserving inlet volume.

The inflow fields retained in a report determined the conservative storage margin. At 54 m³/h and four hours, the median estimate divided by fine-input required storage decreased from 6.50 with volumes alone to 3.34 with peaks and 1.75 with residual extrema. Combining the averaged requirement, nine duration maxima and the residual range enclosed required storage in all 264 record–outflow–block combinations. At one hour, median upper-to-lower ratios were 1.14 and 1.29 at 18 and 54 m³/h. Under constant outflow, these endpoints distinguish sufficient, insufficient and unresolved available storage.

Identical block volumes, peaks and residual extrema permitted different required storage in the controlled inputs, with P2 surface depths of 130.25 and 82.74 mm at the higher loading. Duration-specific maxima distinguished the pair. Across the monitoring records, nine durations alone underestimated storage by up to 44.3%; adding 48 and 96 h reduced that maximum to 10.9%. The combined interval used the sparse estimate as a lower bound while retaining a conservative upper bound.

Capacity sufficiency applies to the reconstructed inlet over the observation horizon, the stated initialization and the specified hydraulic assumptions. The combined interval concerns an initially empty store with constant outflow; it does not establish a return-period design capacity. Agreement in the prescribed nonlinear layered simulations provides numerical evidence for those cases rather than a universal guarantee.

Acknowledgements

We thank the authors of the Wicks Reserve data release for making the monitoring records and measurement definitions publicly available.

REFERENCES

1. Baker, D. B., Richards, R. P., Loftus, T. T., Kramer, J. W. (2004). A new flashiness index: Characteristics and applications to midwestern rivers and streams. *Journal of the American Water Resources Association*, *40*(2), 503–522. https://doi.org/10.1111/j.1752-1688.2004.tb01046.x
2. Białek, A., Musz-Pomorska, A. (2025). Development of a computational tool for stormwater management in small urban catchments. *Journal of Ecological Engineering*, *26*(6), 410–423. https://doi.org/10.12911/22998993/202322
3. Bonneau, J., Fletcher, T. D., Costelloe, J. F., Poelsma, P. J., James, R. B., Burns, M. J. (2020). The hydrologic, water quality and flow regime performance of a bioretention basin in Melbourne, Australia. *Urban Water Journal*, *17*(4), 303–314. https://doi.org/10.1080/1573062X.2020.1769688
4. Bonneau, J., Fletcher, T. D., Lassabatère, L., Lipeme Kouyi, G. (2021). *Inflows, outflows, water levels of Wicks reserve bioretention system for 22 rainfall events* (Version v1) [Data set]. Zenodo. https://doi.org/10.5281/zenodo.4717453
5. Bonneau, J., Lipeme Kouyi, G., Lassabatère, L., Fletcher, T. D. (2021). Field validation of a physically-based model for bioretention systems. *Journal of Cleaner Production*, *312*, 127636. https://doi.org/10.1016/j.jclepro.2021.127636
6. Browne, D., Irani, Z., Galbraith, P., Monetti, J. (2024). *Green infrastructure stormwater retention performance report – Stage 2 calibration* (Version 1.2). e2designlab / Sydney Water. https://www.sydneywater.com.au/content/dam/sydneywater/documents/Green-infrastructure-retention-Stage-2.pdf
7. Bruni, G., Reinoso, R., van de Giesen, N. C., Clemens, F. H. L. R., ten Veldhuis, J. A. E. (2015). On the sensitivity of urban hydrodynamic modelling to rainfall spatial and temporal resolution. *Hydrology and Earth System Sciences*, *19*(2), 691–709. https://doi.org/10.5194/hess-19-691-2015
8. Burns, M. J., Good, K. D., Wani, O. (2026). Influence of weather fronts on design storm profiles: Applied event partitioning and comparative analysis. *Water Resources Research*, *62*(4), e2025WR041528. https://doi.org/10.1029/2025WR041528
9. Castro, C. V., Hung, F., Sivapalan, M. (2025). From scaling theory to stormwater practice: A predictive framework for low impact development planning. *Water Resources Research*, *61*(12), e2025WR040813. https://doi.org/10.1029/2025WR040813
10. Cristiano, E., ten Veldhuis, M.-C., van de Giesen, N. (2017). Spatial and temporal variability of rainfall and their effects on hydrological response in urban areas – a review. *Hydrology and Earth System Sciences*, *21*(7), 3859–3878. https://doi.org/10.5194/hess-21-3859-2017
11. De-Ville, S., Ren, S., Stovin, V. (2025). Bioretention column detention test data for percolation model evaluation. *Urban Water Journal*, *22*(6), 693–705. https://doi.org/10.1080/1573062X.2025.2495874
12. Geosyntec Consultants, & Wright Water Engineers, Inc. (2011). *International Stormwater Best Management Practices (BMP) Database: Technical summary—Volume reduction*. International Stormwater BMP Database. https://bmpdatabase.org/s/2011_VolumeReductionTechnicalSummary.pdf
13. Gomes, M. N., Jr., Giacomoni, M. H., de Macedo, M. B., do Lago, C. A. F., Brasil, J. A. T., de Oliveira, T. R. P., Mendiondo, E. M. (2023). A modeling framework for bioretention analysis: Assessing the hydrologic performance under system uncertainty. *Journal of Hydrologic Engineering*, *28*(9), 04023025. https://doi.org/10.1061/JHYEFF.HEENG-5705
14. Hach Company. (2009). *Sigma 950 flow meter: User manual* (7th ed., Catalog No. 3314). https://cdn.hach.com/7FYZVWYB/at/sw5gc9pfjkcw-p79xj3k8c3b/SIGMA_950_Flow_Meter_Instrument_Manual-3314.pdf
15. Howie, D. C., Milesi, C. (2026). *Technical guidance manual for evaluating emerging stormwater treatment technologies: Technology Assessment Protocol–Ecology (TAPE)* (Publication 18-10-038, March 2026 revision). Washington State Department of Ecology. https://apps.ecology.wa.gov/publications/documents/1810038.pdf
16. Huang, Y., Bárdossy, A., Zhang, K. (2019). Sensitivity of hydrological models to temporal and spatial resolutions of rainfall data. *Hydrology and Earth System Sciences*, *23*(6), 2647–2663. https://doi.org/10.5194/hess-23-2647-2019
17. Kruk, Ł., Lehoczky, J., Ramanan, K., Shreve, S. (2007). An explicit formula for the Skorokhod map on [0, a]. *The Annals of Probability*, *35*(5), 1740–1768. https://doi.org/10.1214/009117906000000890
18. Le Boudec, J.-Y., Thiran, P. (2001). *Network calculus: A theory of deterministic queuing systems for the Internet*. Springer. https://doi.org/10.1007/3-540-45318-0
19. Lisenbee, W. A., Hathaway, J. M., Burns, M. J., Fletcher, T. D. (2021). Modeling bioretention stormwater systems: Current models and future research needs. *Environmental Modelling & Software*, *144*, 105146. https://doi.org/10.1016/j.envsoft.2021.105146
20. Lisenbee, W. A., Hathaway, J. M., Winston, R. J. (2022). Modeling bioretention hydrology: Quantifying the performance of DRAINMOD-Urban and the SWMM LID module. *Journal of Hydrology*, *612*, 128179. https://doi.org/10.1016/j.jhydrol.2022.128179

21. McDonnell, B. E., Ratliff, K., Tryby, M. E., Wu, J. J. X., Mullapudi, A. (2020). PySWMM: The Python interface to Stormwater Management Model (SWMM). *Journal of Open Source Software*, *5*(52), 2292. https://doi.org/10.21105/joss.02292
22. Rossman, L. A., Huber, W. C. (2016). *Storm Water Management Model reference manual: Volume III—Water quality* (EPA/600/R-16/093). U.S. Environmental Protection Agency. https://nepis.epa.gov/Exe/ZyPURL.cgi?Dockey=P100P2NY.TXT
23. Rossman, L. A., Simon, M. A. (2022). *Storm Water Management Model user's manual version 5.2* (EPA/600/R-22/030). U.S. Environmental Protection Agency. https://www.epa.gov/system/files/documents/2022-04/swmm-users-manual-version-5.2.pdf
24. Sambito, M., Rotaru, A. M., Dallan, E., Mazzoglio, P., Treppiedi, D., Lompi, M., Asaridis, P., Maglia, N., Raimondi, A. (2026). Stormwater detention basin design: A review of traditional approaches and current challenges. *International Journal of River Basin Management*, 1–15. https://doi.org/10.1080/15715124.2026.2628347
25. Santos, D. M., Goldenfum, J. A., Dornelles, F. (2021). Outflow adjustment coefficient for the design of storage facilities using the rain envelope method applied to Brazilian state capitals. *Revista Ambiente & Água*, *16*(6), e2707. https://doi.org/10.4136/ambi-agua.2707
26. Tudaji, M., Nan, Y., Tian, F. (2025a). Assessing the value of high-resolution data and parameter transferability across temporal scales in hydrological modeling: A case study in northern China. *Hydrology and Earth System Sciences*, *29*(12), 2633–2654. https://doi.org/10.5194/hess-29-2633-2025
27. Tudaji, M., Nan, Y., Tian, F. (2025b). Assessing the value of high-resolution rainfall and streamflow data for hydrological modeling: An analysis based on 63 catchments in southeast China. *Hydrology and Earth System Sciences*, *29*(7), 1919–1937. https://doi.org/10.5194/hess-29-1919-2025
28. U.S. Environmental Protection Agency. (2021). *Stormwater best management practice: Bioretention (rain gardens)* (EPA-832-F-21-031L). https://www.epa.gov/system/files/documents/2021-11/bmp-bioretention-rain-gardens.pdf
29. Wang, J., Chua, L. H. C., Shanahan, P. (2019). Hydrological modeling and field validation of a bioretention basin. *Journal of Environmental Management*, *240*, 149–159. https://doi.org/10.1016/j.jenvman.2019.03.090
30. Wright Water Engineers, Inc., & Geosyntec Consultants. (2019). *International Stormwater Best Management Practices (BMP) Database: User's guide for urban stormwater BMP data entry spreadsheets* (Version 4.0). Water Research Foundation. https://bmpdatabase.org/s/2019_BMPDatabaseUsersGuide.pdf